Stress tensor inversions in the Northern Egypt

By
Asem Salama

PhD student at Eost-IPG-CNRS 7516 Strasbourg,
Assistant researcher at NRIAG

In collaboration with
Mustapha Meghraoui, Hesham Hussein, Mohamed El Gabry

Outlines

- Sesimotectonics in the north Egypt
- Active zones in northern Egypt
- Stress tensor inversion of focal mechanisms in the six active zones of northern Egypt.
- Stress pattern in the African continent

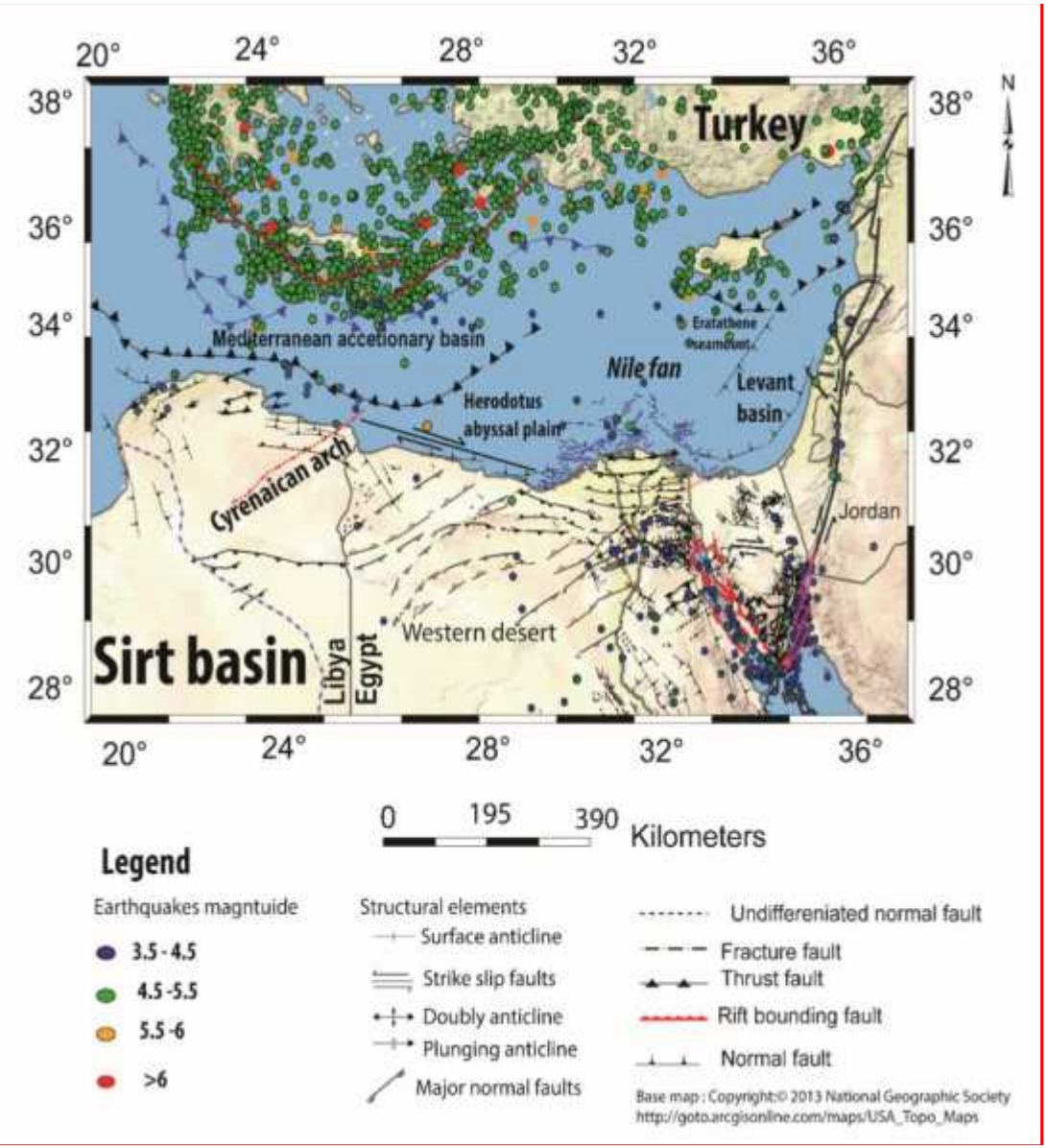

Seismic activity and tectonic map based on (a geological map of Libya, 1985 geological map of Egypt EMRA, 2008; Bathworth, 2008) and seismicity data for north Egypt of NRIAG bulletin from 1997-2016 and the seismicity data of the Eastern Mediterranean from IRIS bulletin

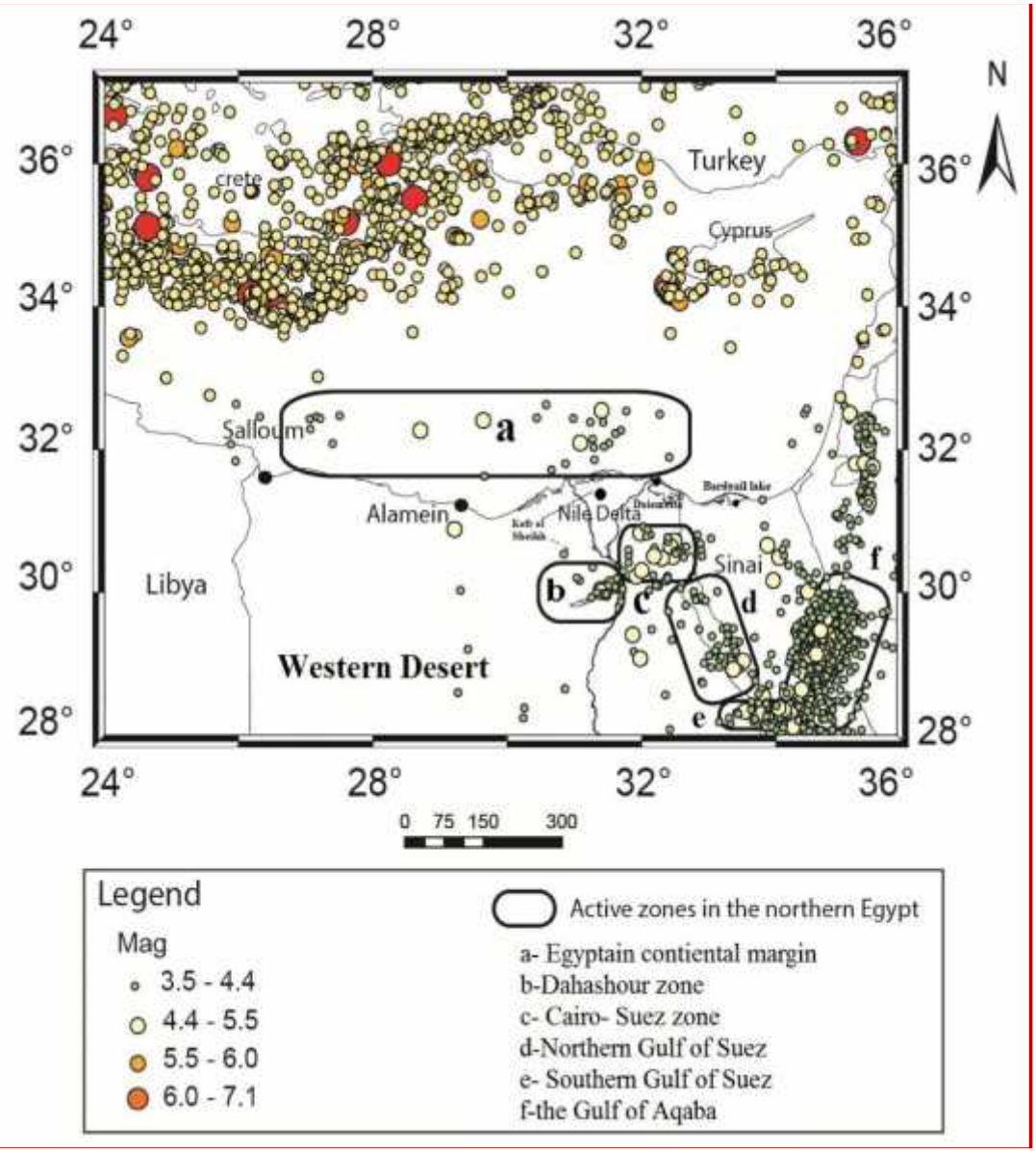

The active zones of northern Egypt and seismicity (Mag. ≥ 3.5) based on NRIAG and IRIS seismicity bulletins.

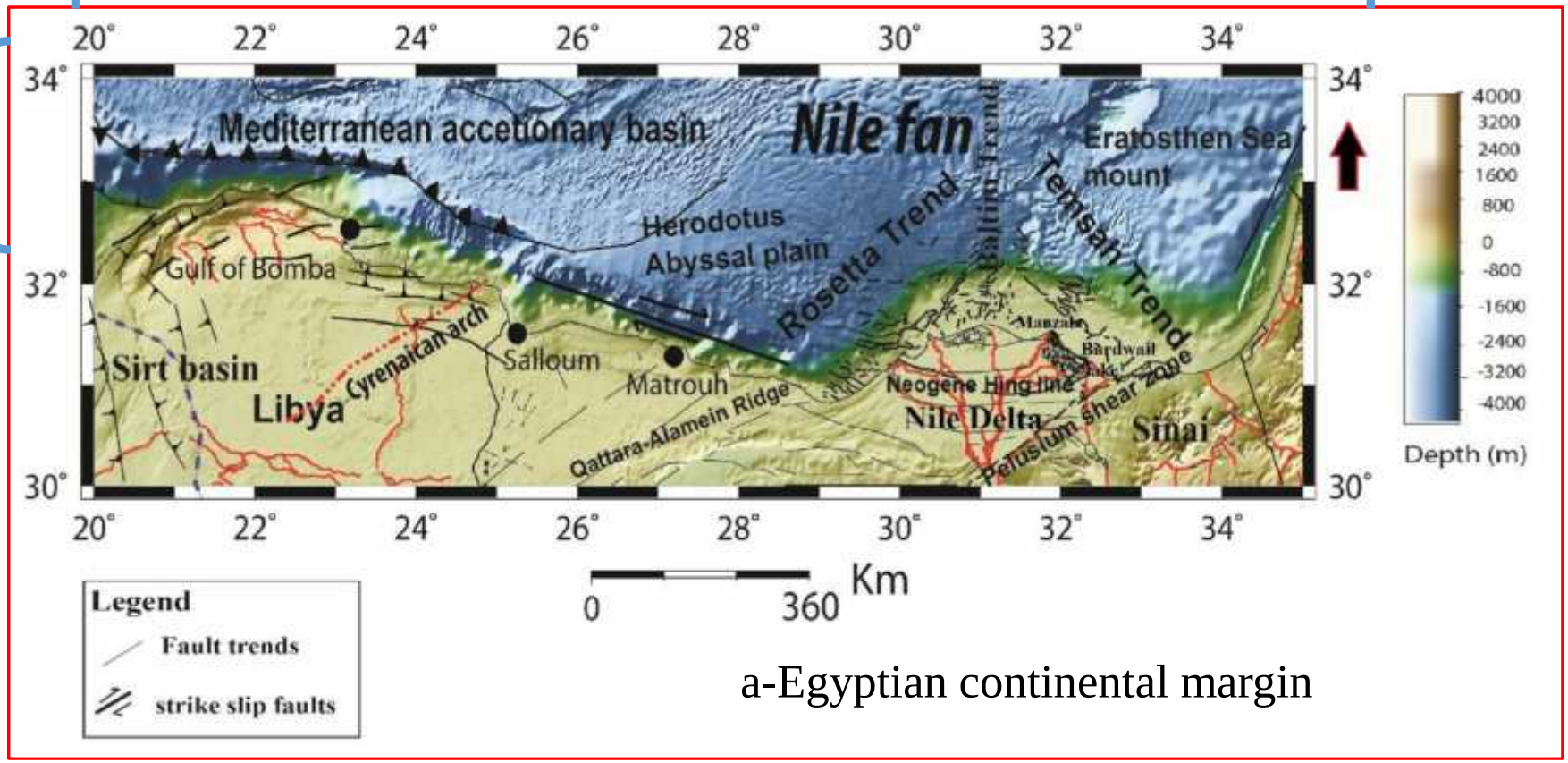

a-Egyptian continental margin

Northern Egyptian continental margin with major simplified geological structures onshore and offshore (Abdel Aal et al.1994; Egyptian geological map EMRA, 2008); bathymetry data of ETOPO1 (1 min-arc)

Geology and Tectonic setting
(Abdel Aal et al.1994)

First Phase

-Late Paleozoic and Early Mesozoic

(650-208 Ma)

Results in

E-W trending faults (bisects Sinai and Western Desert and including hing zone of the Nile Delta

Other trending:

a- NE-SW to ENE- WSW trending, either normal or strike slip left lateral movement in northern Egypt

b- NE trending of Rosetta normal faulting system extended to the northwestern desert of Qattara –El Alamein ridge

Second Phase

Late Cretaceous – Early Tertiary
(145-33 Ma)

NW-SE oblique compression (closing of Tethys Sea)

Results in
a- 'echelon' NE-SW trending ,
b- double anticline belt (Syrian arc) and its extension from north Sinai to Abu Roash in western Desert.

c- NW to NNW extension parallel to the major compression motion affected the north Egypt

Third Phase

Late Eocene to recent times
(33.7 Ma-recent times)

Opening of Red Sea; Gilf of Suez rifting

Results in
a- Gulf of Suez NNW normal faults also observed in Nile Delta

b- NNE development in Gulf of Aqaba during Mioscene

c- N-S Baltim faults formed during rejuvenation of olders pretertiary during Mioscene

Egyptian continental margin Zone A (Trend A & Trend B)

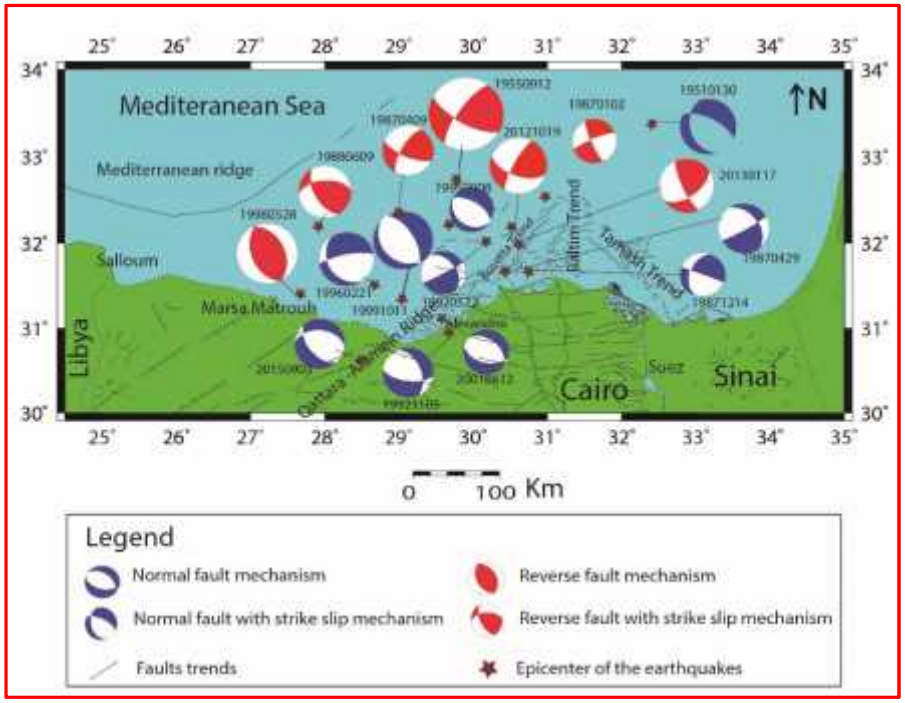

The chosen approach is based on the Tensor (version 5.8.6 of 23/11/2016) program of Delvaux and Sperner (2003). R= R = (σ2 - σ3)/(σl - σ3)

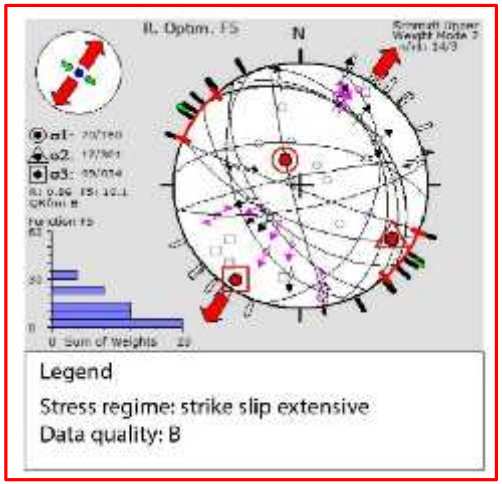

Zone A, Trend A, rotational optimization method applied to 10 focal mechanisms

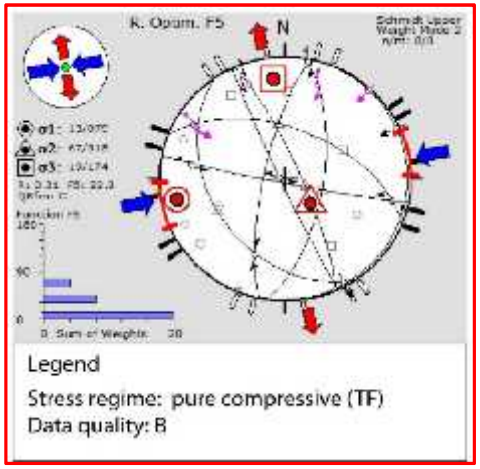

Zone A, Trend B, rotational optimization method applied to 10 focal mechanisms

Dahshour, Zone B

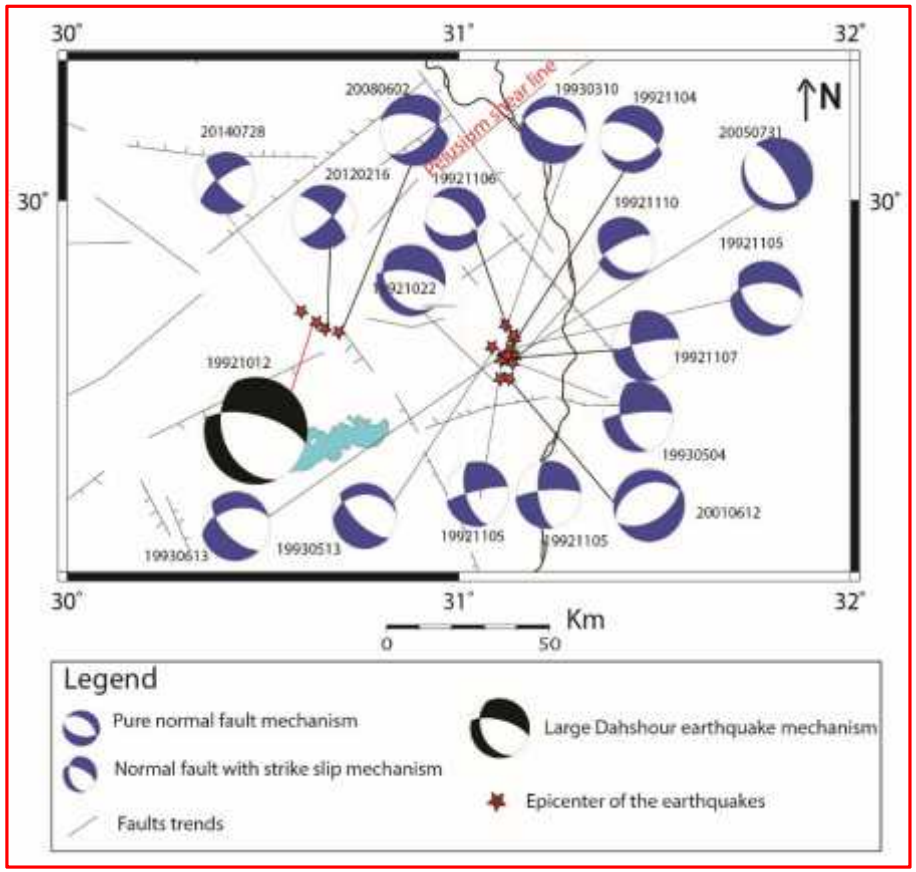

Focal mechanisms of 15 events $M_L \geq 3.5$ at the Dahshour area, NE-SW trending faults

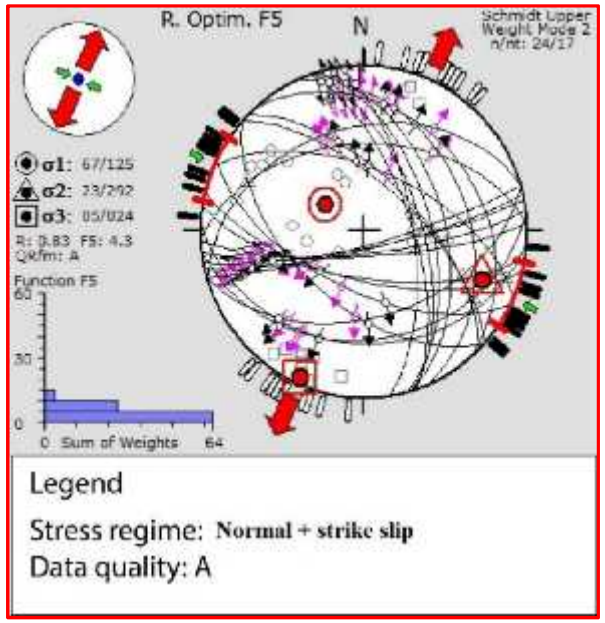

Dahshour ; Zone B, rotational optimization method the present day stress tensor applied to 13 focal mechanisms.

Cairo – Suez zone , Zone C

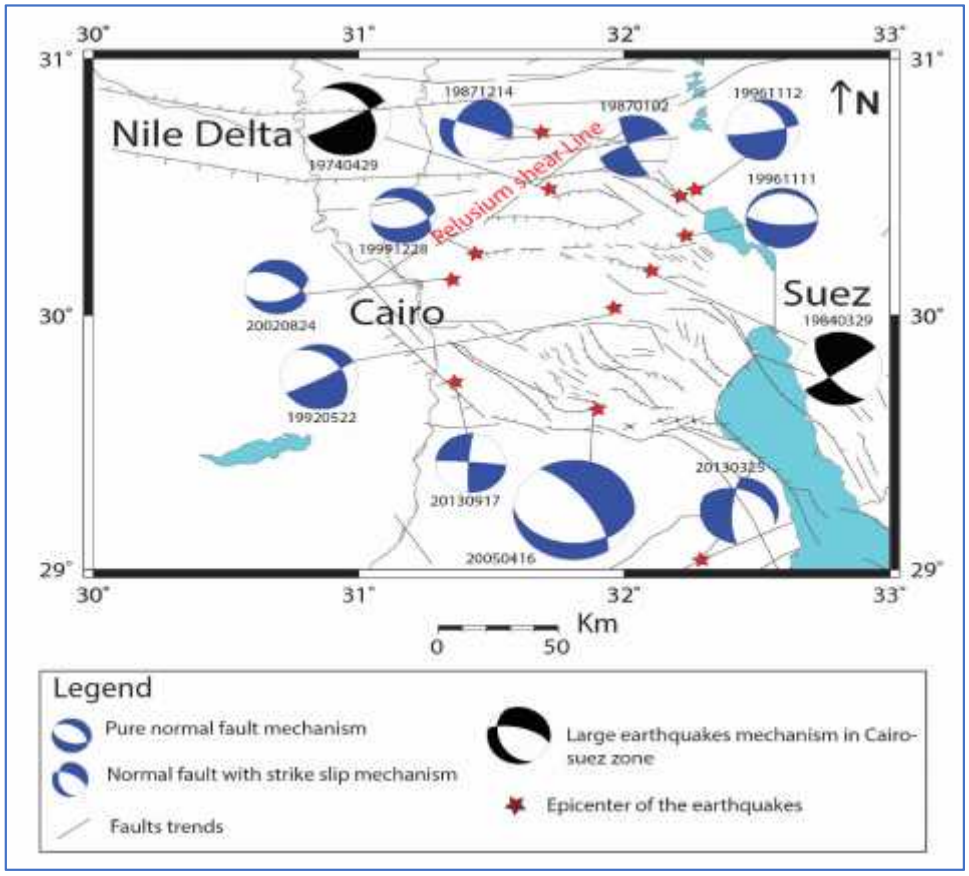

Focal mechanisms of 12 events with $M_L \geq 3.5$ magnitude in Cairo-Suez area

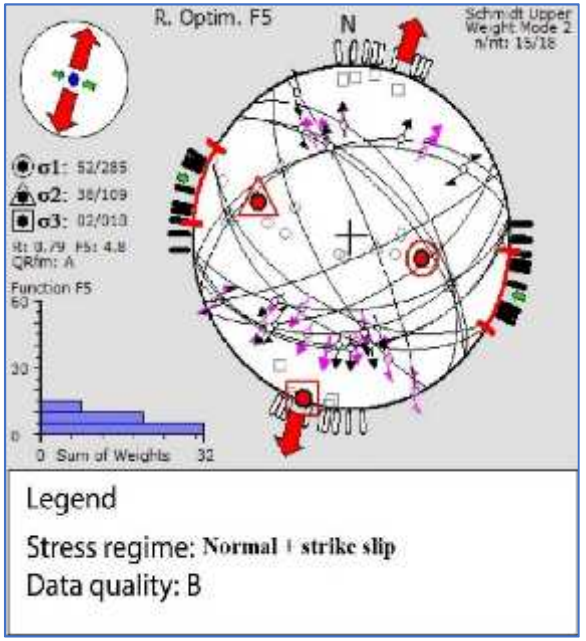

Cairo-Suez zone, Zone C, rotational optimization method of the present day stress tensor deduced from 12 focal mechanisms data

Northern Gulf of Suez zone, Zone D

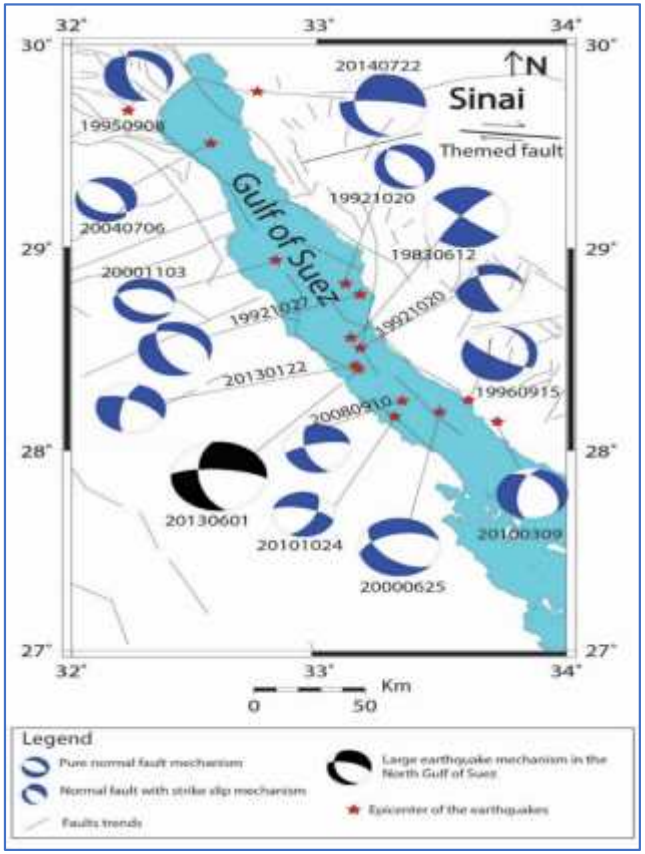

Focal mechanisms of 15 earthquakes with $M_L \geq$ 3.5 magnitude in the northern of Gulf of Suez

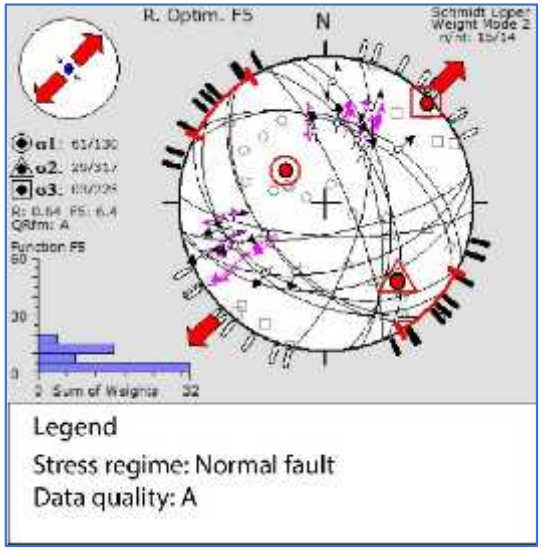

Northern Gulf of Suez, Zone D, rotational optimization method of the present day stress tensor deduced from 14 focal mechanisms

Southern Gulf of Suez zone, Zone E

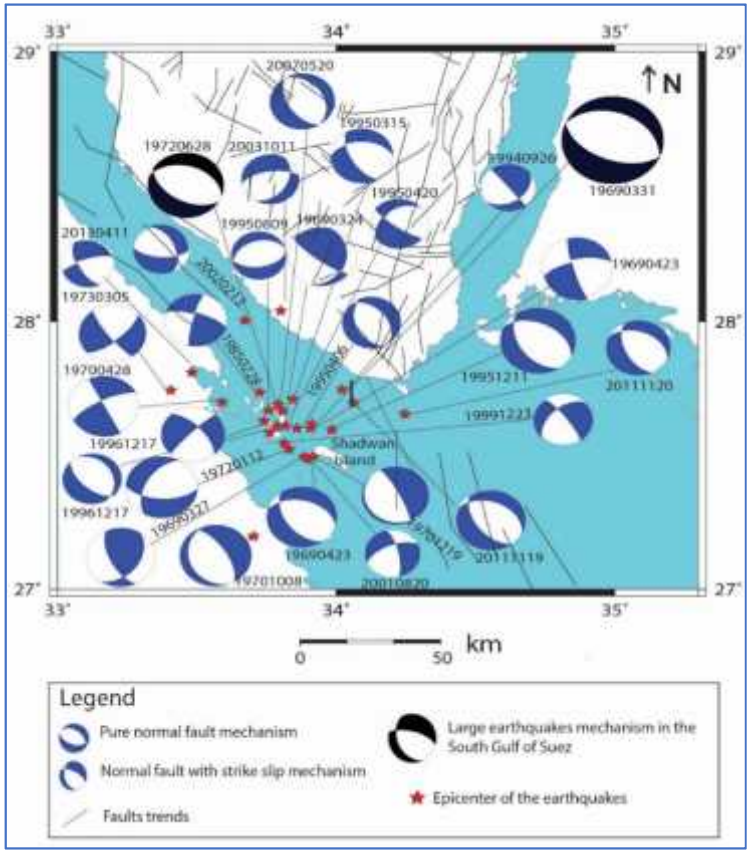

Focal mechanisms of 29 earthquakes with $M_L \geq 3.5$ magnitude in the Southern of Gulf of Suez, Zone E

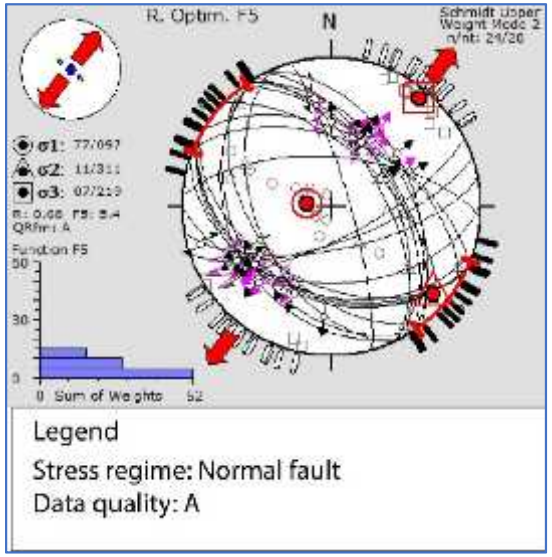

Southern Gulf of Suez, Zone E ,rotational optimization method of the present day stress tensor deduced from 28 focal mechanisms

Gulf of Aqaba (subzone F, G)

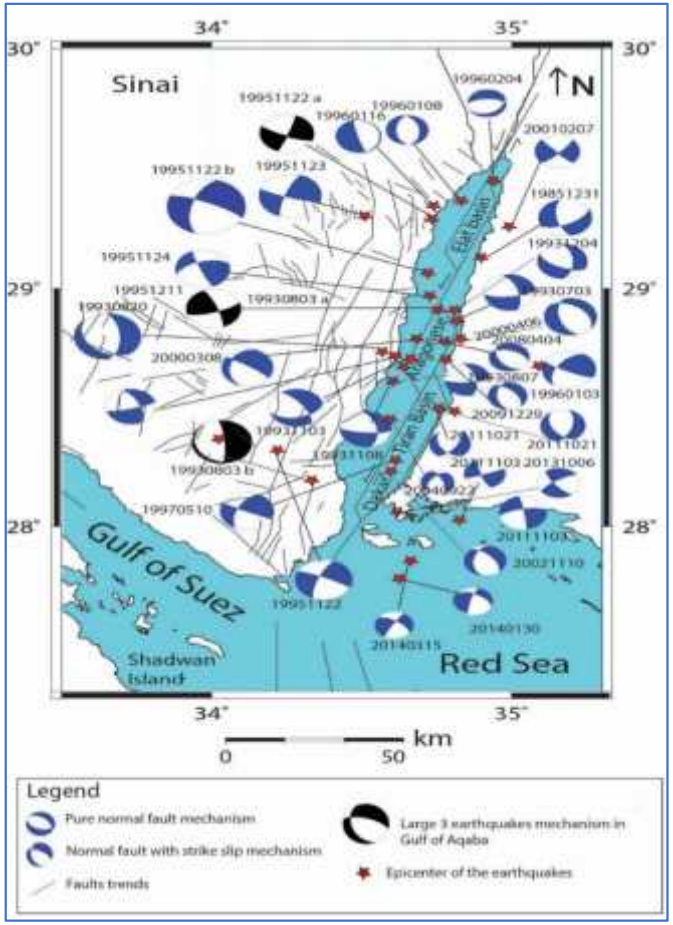

subzone F

subzone G

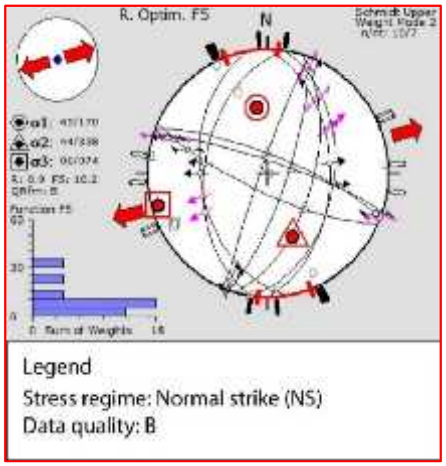

Gulf of Aqaba, subzone F rotational optimizations methods of the present day stress tensor deduced from 7 focal mechanisms.

Gulf of Aqaba, subzone G, rotational optimization methods of the present day stress tensor deduced from 24 focal mechanisms

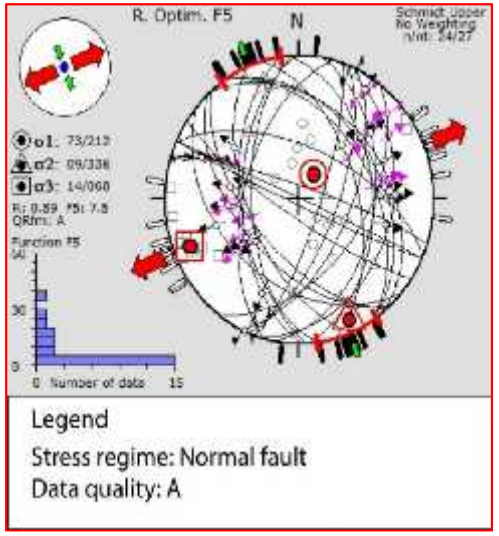

Focal mechanisms of 36 earthquakes with $M_L \geq 3.5$ magnitude in the Gulf of Aqaba , Subzone F, G

Table 1 summarized the calculated stress inversion in the northern active zones in northern Egypt

Seismic zone	**σ1**		**σ 2**		**σ 3**		**R**	**α º**	**α º max**	**n/nt**	**R'**	**Shmax.º**	**Shminº**
	Az.	Pl.	Az.	Pl.	Az	Pl.							
Continental margin Zone A Trend A	74	168	13	313	09	45	0.79	18.4	33.4	14/18	0.67	136	39.2
Continental margin Zone A Trend B	10	67	04	336	79	255	0.12	6.1	20.8	8/16	2.12	79	165
Dahshour Zone B	67	125	23	292	05	24	0.83	18.3	22.4	24/34	0.69	114	N25E
Cairo- Suez Zone C	63	286	27	108	01	18	0.79	10.7	20.8	15/36	0.69	108	N18.7E
North Gulf of Suez Zone D	61	130	29	317	03	225	0.64	12	24.9	15/28	0.64	134	44
South Gulf of Suez Zone E	77	97	11	311	07	219	0.68	11	23.8	24/56	0.51	128	27.8
Gulf of Aqaba sub zone F	45	170	44	338	06	74	0.9	13.5	26.8	10/14	0.98	164	72.3
Gulf of Aqaba sub zoneG	09	212	09	336	14	68	0.89	11.4	38.6	24/54	0.89	161	68.3

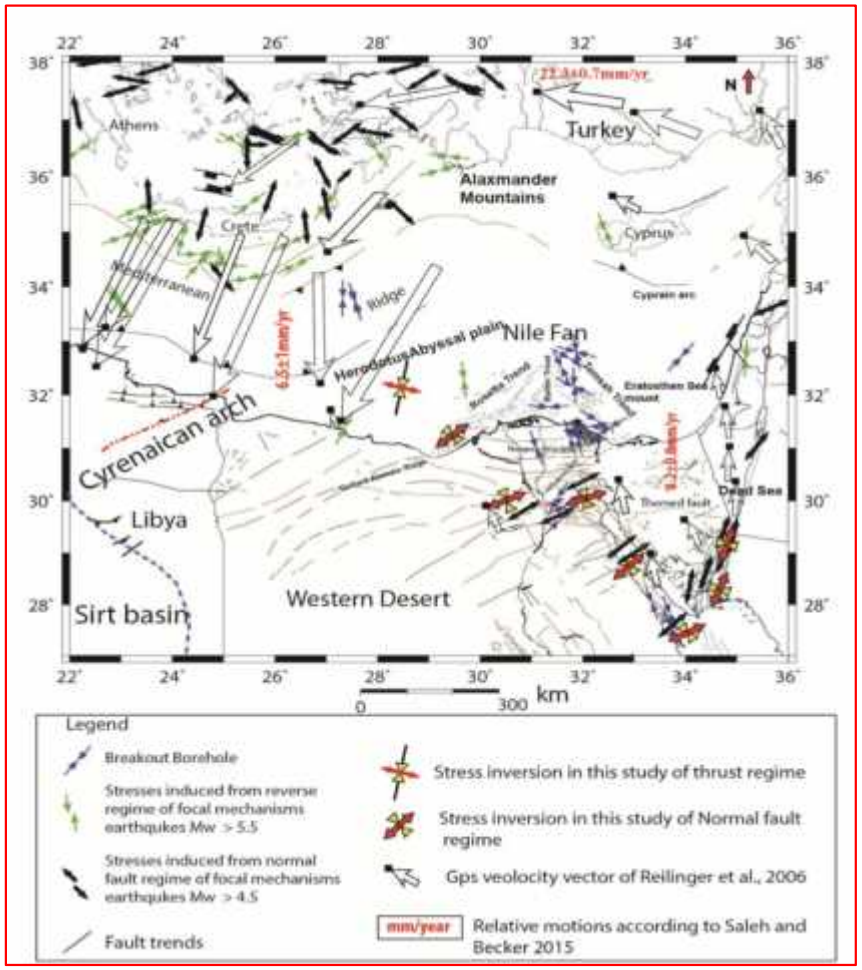

Stress map of the North Egypt and Eastern Mediterranean region

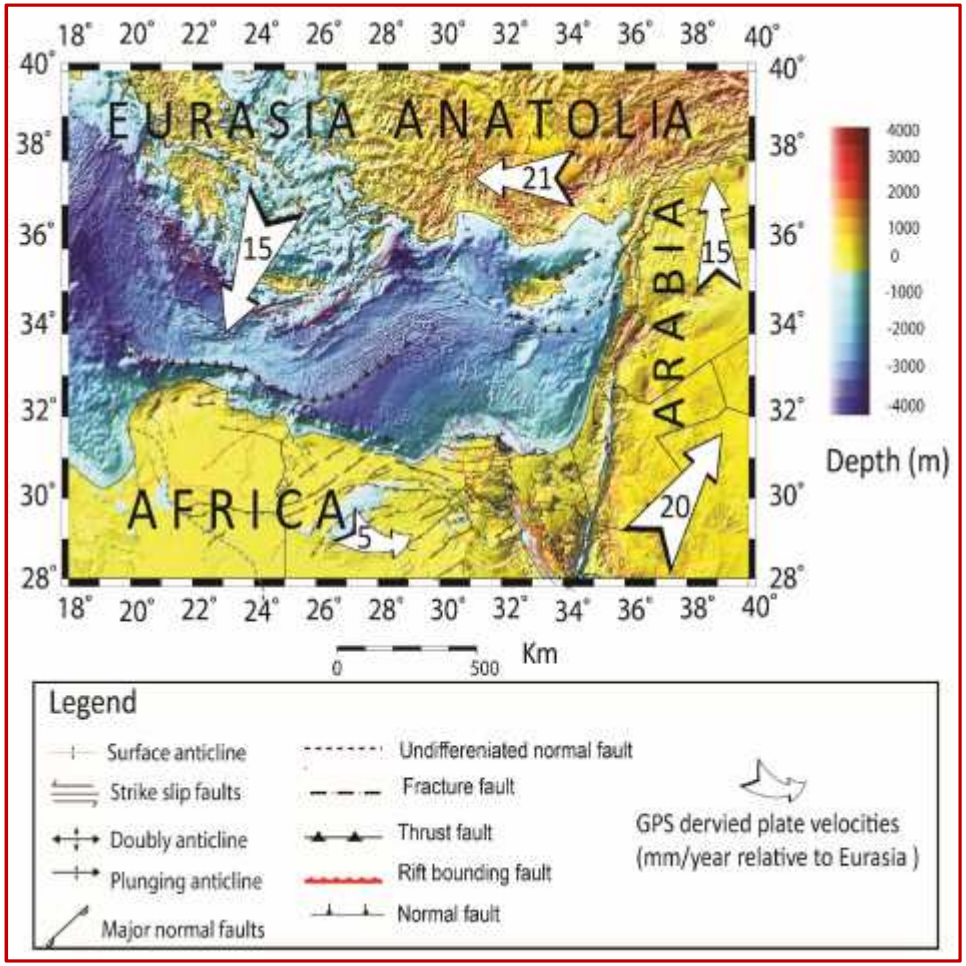

Morphotectonic map of the Mediterranean with major, data from GPS (Reilinger et al., 2006)

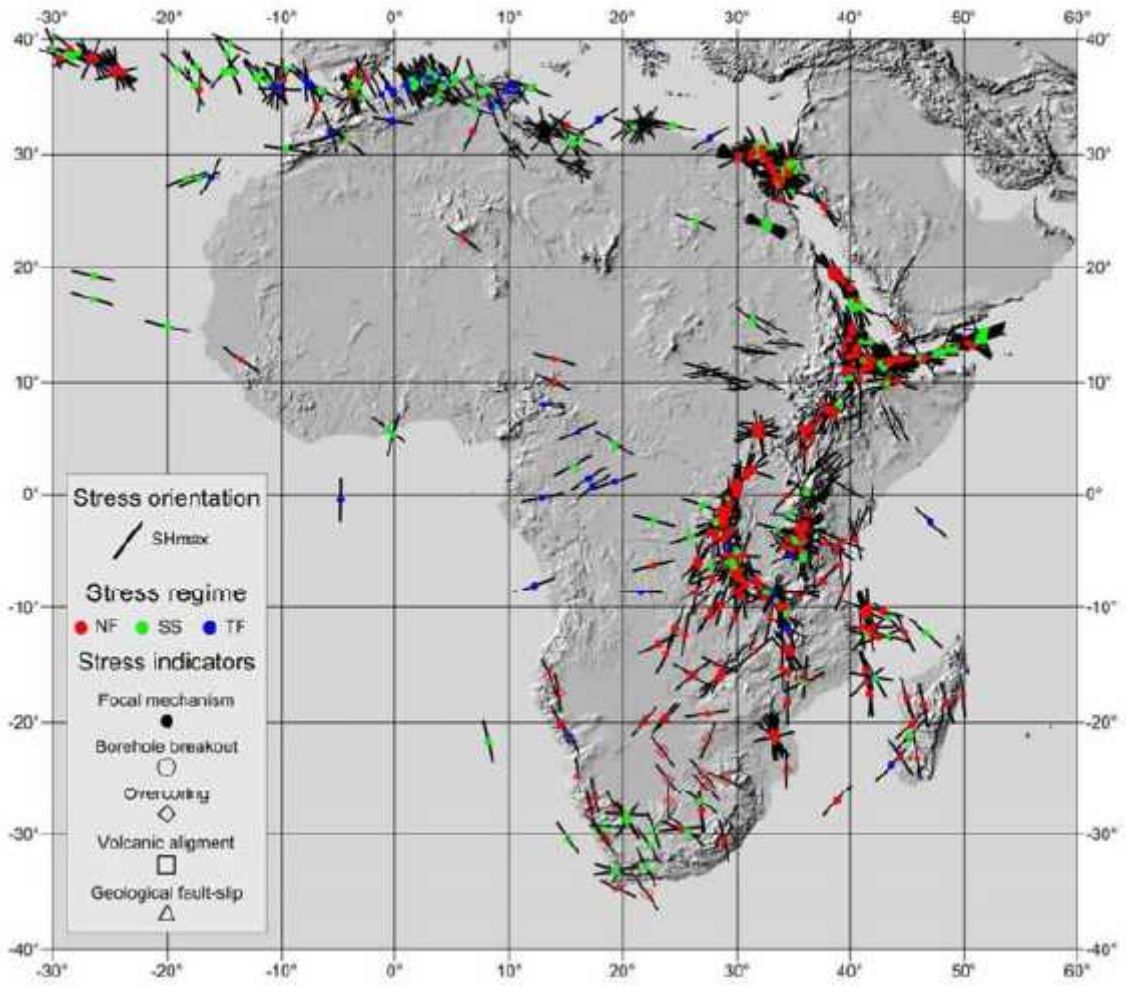

Stress map of the African; Meghraoui et al., 2016

Conclusions

1-The stress inversion results of north Egypt are obtained by using the Tensor program version 5.8.6 of 23/11/2016 by Delvaux and Sperner 2003 for the six active zones in the north Egypt.

2- The stress Tensor results shows that the whole northern Egypt is under extensional stress in the five active zone except the Egyptian continental margin.

a- Egyptian content ail margin Zone A trend A& B (R'= 0.67 & 2.12)
b- Dahshour Zone B (R'= 0.69)
c-Cairo Suez Zone C (R'= 0.69)
d-Northern Gulf of Suez (R'= 0.64)
e-Southern Gulf of Suez (R'= 0.51)
f- Gulf of Aqaba subzone F & G (0.98 & 0.89)

3- Our stress calculated results are coincide with stresses determined in the North east Africa continent.

Thanks